

# Ground state properties of ferromagnetic metal/conjugated polymer interfaces

S. J. Xie<sup>1,2</sup>, K. H. Ahn<sup>1</sup>, D. L. Smith<sup>1</sup>, A. R. Bishop<sup>1</sup>, and A. Saxena<sup>1</sup>

<sup>1</sup>Theoretical Division, Los Alamos National Laboratory, Los Alamos, New Mexico 87545

<sup>2</sup>School of Physics and Microelectronics, Shandong University, Jinan, 250100, Peoples Republic of China

(March 22, 2024)

## Abstract

We theoretically investigate the ground state properties of ferromagnetic metal/conjugated polymer interfaces. The work is partially motivated by recent experiments in which injection of spin polarized electrons from ferromagnetic contacts into thin films of conjugated polymers was reported. We use a one-dimensional nondegenerate Su-Schrieffer-Heeger (SSH) Hamiltonian to describe the conjugated polymer and one-dimensional tight-binding models to describe the ferromagnetic metal. We consider both a model for a conventional ferromagnetic metal, in which there are no explicit structural degrees of freedom, and a model for a half-metallic ferromagnetic colossal magnetoresistance (CMR) oxide which has explicit structural degrees of freedom. The Fermi energy of the ferromagnetic metal contact is adjusted to control the degree of electron transfer into the polymer. We investigate electron charge and spin transfer from the ferromagnetic metal to the organic polymer, and structural relaxation near the interface. Bipolarons are the lowest energy charge state in the bulk polymer for the nondegenerate SSH model Hamiltonian. As a result electrons (or holes) transferred into the bulk of the polymer form spinless bipolarons. However, there can be spin density in the polymer localized near

the interface.

PACS numbers: 72.25.-b, 73.61.Ph, 75.30.Vn, 71.38.-k

## I. INTRODUCTION

Magnetoelectronics or spintronics is a field of growing interest. Since the discovery of giant magnetoresistance (GMR) [1], rapid progress has been made in this field. Electron spin injection and spin dependent transport are essential aspects of spintronics and have been extensively studied in a number of different contexts including: ferromagnetic metals to superconductors [2]; ferromagnetic metals to normal metals [3]; ferromagnetic metals to nonmagnetic semiconductors [4] and magnetic semiconductors to nonmagnetic semiconductors [5]. Recently, spin polarized injection and spin polarized transport in conjugated polymers have been reported [6]. Specifically, spin injection was observed into thin films of the conjugated organic material sexithienyl from half-metallic manganites (in which electron spins at the Fermi surface are completely polarized) at room temperature. The ease of fabrication and low temperature processing of conjugated organic materials open many application possibilities, and electronic as well as opto-electronic devices fabricated from these materials, e.g. organic light-emitting diodes and spin valves, are being actively pursued [6].

Theoretical study of spin polarized injection and transport has been carried out primarily in the framework of classical transport equations [7-9]. The role of interface properties for spin injection in inorganic semiconductors was investigated in this context [10-13]. The purpose of this paper is to study the ground state characteristics such as lattice displacements, charge density and spin density distribution of conjugated organic polymers contacted with a ferromagnetic metal. An added motivation to study this type of "active" interface is that because of relatively large electron-phonon coupling the materials on both sides of the interface can deform, which may facilitate spin polarized injection.

The paper is organized as follows. In the next section we present tight-binding models for a nondegenerate conjugated polymer, a ferromagnetic (FM) metal, a half-metallic colossal magnetoresistance (CMR) material and the interface between the polymer and the two kinds of magnetic materials. Section III presents the results for a model junction between the polymer and the FM metal, and Sec. IV describes results for CMR/polymer junctions.

Our main findings are summarized in Sec. V.

## II. MODEL

Organic polymers currently used for electronic and opto-electronic devices typically have a nondegenerate ground state. The first experimental evidence of spin polarized electrical injection and transport in conjugated organic materials was carried out using sexithienyl (T<sub>6</sub>), a  $\pi$ -conjugated oligomer [6,14]. The underlying physics of spin injection and transport is of particular interest for conjugated organic materials, where strong electron-phonon coupling leads to polaronic (or bipolaronic) charged states [15]. These polymers or oligomers have chain structures that can be described using a nondegenerate version of the one-dimensional SSH model, the Brazovskii-Kirova (BK) model [16,17],

$$H_P = \sum_i \epsilon_P a_{i,\uparrow}^\dagger a_{i,\uparrow} + \sum_i [t_P - t_1 (-1)^i] a_{i+1,\uparrow}^\dagger a_{i,\uparrow} + \sum_i \frac{1}{2} K_P (u_{i+1} - u_i)^2; \quad (1)$$

where  $a_{i,\uparrow}^\dagger$  ( $a_{i,\uparrow}$ ) denotes the electron creation (annihilation) operator at site  $i$  with spin  $\uparrow$ ,  $\epsilon_P$  is the on-site electron energy of an atom,  $t_P$  is the transfer integral in a uniform (undimerized) lattice and  $\epsilon_P$  the electron-phonon interaction parameter,  $t_1$  introduces nondegeneracy into the polymer, and  $K_P$  denotes a spring constant.

To describe a conventional ferromagnetic metal we use a one-dimensional tight-binding model with kinetic energy ( $H_{ke}$ ) and spin splitting ( $H_{Hund}$ ) terms:

$$H_{FM} = H_{ke} + H_{Hund}; \quad (2)$$

$$H_{ke} = \sum_i t_F (a_{i,\uparrow}^\dagger a_{i+1,\uparrow} + a_{i+1,\downarrow}^\dagger a_{i,\downarrow}); \quad (3)$$

$$H_{Hund} = \sum_i J_i (a_{i,\uparrow}^\dagger a_{i,\uparrow} - a_{i,\downarrow}^\dagger a_{i,\downarrow}); \quad (4)$$

where  $t_F$  is the transfer integral for a ferromagnetic metal and  $H_{Hund}$  describes the spin splitting of the magnetic atom with site-dependent strength  $J_i$ . We take an occupation of

one electron per atom and  $J_1 = J_M$  with parameters  $t_F = 0.622$  eV and  $J_M = 0.625$  eV for the conventional ferromagnetic metal.

CMR materials can form half-metallic ferromagnets and are therefore very interesting as spin polarized electron injecting contacts. CMR materials have a chemical composition such as  $Re_{1-x}Ak_xMnO_3$ , where Re represents a rare earth atom, e.g. La and Nd, and Ak represents an alkali metal such as Ca, Sr and Ba. Mn has a valence of  $(3+x)$  which depends on the doping concentration  $x$ . Depending on doping, the material can be either a metal or an insulator and either ferromagnetic or antiferromagnetic [18]. In particular,  $Re_{1-x}Ak_xMnO_3$  can be a half-metallic ferromagnet when  $0.2 < x < 0.5$ , for example, with Re=La and Ak=Ca. In this state all the electrons at the Fermi surface have the same spin orientation. The Mn atom has 5 electrons in its 3d orbitals. These electrons have a parallel spin alignment due to a strong Hund's rule splitting. Because of crystal field splitting in a solid, three of the orbitals form the low energy  $t_{2g}$  states,  $xy$ ,  $yz$  and  $zx$ , and the other two form the higher energy  $e_g$  states,  $x^2 - y^2$  and  $3z^2 - r^2$ . In the ground state, the electrons in  $t_{2g}$  are localized and constitute core spins. The  $e_g$  states are extended and the electrons in these states can be delocalized. In cubic symmetry, the two  $e_g$  levels are degenerate. However in tetragonal or orthorhombic symmetry, the degeneracy of  $e_g$  is broken by a Jahn-Teller coupling due to the electron-lattice interaction, which causes movement of oxygen ions with respect to the manganese ions.

Here, we suppose for simplicity that a polymer or oligomer chain is connected at the ends of a CMR lattice in the  $z$ -direction. We consider a one-dimensional model which contains the basic properties of a half-metallic CMR material; a ferromagnetic metal with electron-lattice coupling. The following one-dimensional model captures these essential features,

$$H_{CMR} = H_{ke} + H_{Hund} + H_{el-lat} + H_{elastic}; \quad (5)$$

where  $H_{ke}$  and  $H_{Hund}$  are given in Eqs. (3) and (4), and

$$H_{el-lat} = \sum_{i,j}^X F(u_{i+1} - u_i) a_{i,j}^+ a_{i,j}; \quad (6)$$

$$H_{\text{elastic}} = \sum_i \frac{1}{2} K_F [(u_i - u_{i+1})^2 + (u_{i+1} - u_i)^2]; \quad (7)$$

Here  $u_i$  and  $v_i$  are the displacements of the  $i$ th oxygen atom and manganese atom, respectively.  $H_{\text{ke}}$  describes electron hopping between two nearest manganese atoms.  $H_{\text{Hund}}$  describes the spin splitting of a magnetic manganese atom that results from interaction with the core spins. We have  $J_i = J_M$  for the ferromagnetic state (core spins aligned) and  $J_i = (-1)^i J_M$  for the antiferromagnetic state.  $H_{\text{el-lat}}$  gives the on-site energy of the manganese atoms, which depends on the displacement of the nearest neighbor oxygen atoms, and  $K_F$  denotes the electron-lattice coupling strength. The last term  $H_{\text{elastic}}$  represents the elastic energy and includes nearest neighbor interactions.

Coupling at the interface between the conjugated polymer and the ferromagnetic metal is described by the hopping integral,

$$t_{F-P} = (t_F + t_P)/2; \quad (8)$$

where  $\alpha$  is a weighting parameter. In principle, this coupling could be spin-dependent, but here we take  $t_{F-P}^{\uparrow} = t_{F-P}^{\downarrow} = t_{F-P}$  for simplicity. Periodic boundary conditions are adopted.

The parameters used for the CMR contact  $\text{Re}_{1-x}\text{A}_x\text{MnO}_3$  are  $t_F = 0.622$  eV,  $J_M = 1.25$  eV,  $K_F = 7.4$  eV/Å<sup>2</sup> [19] and  $K_P = 2.0$  eV/Å. For the organic polymer we take representative parameters as  $t_P = 2.5$  eV,  $K_P = 4.2$  eV/Å,  $K_P = 21.0$  eV/Å<sup>2</sup> [20]. We set the degeneracy breaking parameter  $t_1 = 0.04$  eV so that the energy difference is  $\epsilon_{AB} = 0.035$  eV per carbon atom between the two dimerized phases. The relative chemical potential  $\mu_P$  was used to adjust the electron transfer between the ferromagnet and the polymer. Segment lengths were taken so that  $\text{Re}_{1-x}\text{A}_x\text{MnO}_3$  consists of 100 MnO units and the polymer 100 of CH units, that is  $N_M = N_P = 100$ . For the most part, the results do not depend on the lengths of the segments if they are not too short (i.e., much longer than the characteristic polaron size). The interfacial coupling parameter was taken as  $\alpha = 1$ . If  $\alpha > 1$ , the interface acts as a potential well and tends to confine electrons, whereas if  $\alpha < 1$  the interface acts as a potential barrier and tends to exclude electrons.

We first study an isolated  $\text{Re}_{1-x}\text{Ak}_x\text{MnO}_3$  chain to test the effectiveness of this model for the CMRM material. The electronic eigenstates

$$|j\rangle = \sum_i^X |Z_{ij}; a_{ij}^+ j\rangle \quad (9)$$

corresponding to the eigenvalue  $\epsilon_j$ , are solved from the equation,

$$t_F |Z_{i+1}; \sigma\rangle - t_F |Z_{i-1}; \sigma\rangle + J_i |Z_{ij}; \sigma\rangle - F (u_{i+1} - u_i) |Z_{ij}; \sigma\rangle = \epsilon_j |Z_{ij}; \sigma\rangle \quad (10)$$

where  $\sigma = +1$  for spin up and  $-1$  for spin down. The displacements  $f_{ij}$  and  $fu_{ij}$  in the ground state are determined from the eigenstates self-consistently:

$$f_{ij} = \frac{1}{2} (u_i + u_{i+1}); \quad (11)$$

$$u_i = \frac{1}{2} \left[ f_{i-1} + f_i - \frac{F}{K_F} \sum_j (Z_{ij}; Z_{ij}; -Z_{i-1j}; Z_{i-1j};) \right]; \quad (12)$$

If  $F = 0$ , the stable configuration has a uniform structure, i.e.  $f_{ij} = 0$  and  $u_i = 0$ , without distortion. Otherwise, some distortion will occur. From Eqs. (11) and (12) we see that the displacements of both oxygen and manganese atoms depend on the electronic density at the manganese atoms.

The structure and magnetism of  $\text{Re}_{1-x}\text{Ak}_x\text{MnO}_3$  depend on the doping concentration  $x$  which determines the electron number per manganese atom. The orbitals of each manganese atom have been renormalized to a single orbital in the present model and the electron number per manganese atom is denoted by  $y$  ( $0 \leq y \leq 1$ ). Figure 1(a) shows the dependence of the energy difference per site between the ferromagnetic (FM) and antiferromagnetic (AFM) states on  $y$ . For an electronic doping concentration  $y = 0$  (no electrons), the FM and AFM states have the same energy and the equilibrium conditions give  $f_{ij} = u_i = 0$ . For  $y = 1$ , that is each manganese atom having one electron, the AFM state is lower in energy than the FM state. An energy gap of 2.5 eV appears in the AFM state for both the spin up and down energy levels. The lower subband levels are occupied and the system is an insulator. At  $y = 0.5$ , the FM state is lower in energy than the AFM state. At this electron concentration,

the energy difference between FM and AFM states is 0.127 eV per manganese atom. In this case, as shown in Fig. 1 (b), the energy bands of the FM state are totally spin split. There is a gap of 0.26 eV at the wavevector  $k = \pi/2a$  ( $a$  is the lattice constant between two nearest Mn sites) and the system is an insulator. This gap can be adjusted by changing  $\mu_F$ . When  $\mu_F = 1.4$  eV/A, the gap is close to zero. All the spin down levels are empty and only the lower sublevels of the spin up band are occupied. At  $y = 0.5$ , the charge density has an oscillatory distribution. For example, at  $\mu_F = 2.0$  eV/A, the densities on two adjacent manganese atoms are about 0.621e and 0.379e (at  $y = 0.5$ ). Away from  $y = 0.5$ , the energy gap disappears and the system becomes a ferromagnetic half metal. In the ferromagnetic state, the sites displace in the approximate pattern,

$$v_i = v_0 \sin[2\pi(y - 0.5)]; \quad (13)$$

$$u_i = u_0 \cos[2\pi(y - 0.5)]; \quad (14)$$

With electron concentration 0.2 ( $y = 0.45$ ), the displacements of both Mn and O atoms become very small ( $v_0 = 0.005$  Å and  $u_0 = 0.01$  Å) and decrease to zero when the chain length becomes arbitrarily long. That is, the system becomes uniform in this doping region, and correspondingly the charge density is also uniform with a half-metallic property. These results are consistent with the basic properties of the CMR materials [18] and show that the one-dimensional model gives a reasonable description of them.

### III. FERROMAGNETIC METAL/POLYMER JUNCTION

We first consider a polymer chain contacted by a simple rigid ferromagnetic metal chain. In the case of half filling for the parameters used, the spin polarization is  $\sigma = (N_{\uparrow} - N_{\downarrow})/(N_{\uparrow} + N_{\downarrow}) = 0.34$ . The polymer has a one-dimensional chain structure with a strong electron-lattice interaction that will cause localized charged excitations. When the polymer is connected with a ferromagnetic metal, both the lattice configuration and charge distribution of the polymer are affected. By adjusting the relative chemical potential, electrons (or holes)



are transferred into the polymer and cause the displacement of the lattice sites. Results are shown in Fig. 2 and Fig. 3 for  $\mu_p = 0$  and  $\mu_p = 1.0$  eV, respectively. Following the usual convention, in this paper the displacement is plotted with a multiplying factor  $(-1)^i$ , where  $i$  is the site index. The ferromagnetic metal is to the left and the polymer is to the right of the interface which is between sites  $n=100$  and  $101$ . In Fig. 2, there is no electron transfer between the segments, and the charge density is uniform within the whole system. But the charges near the interface can be spin polarized. The polarization oscillates and decays into the polymer segment. The decay length of the spin polarization is about  $6b$ , where  $b$  is the lattice constant in the polymer. If the chemical potential of the ferromagnet is higher than the bipolaron level in the polymer, as in Fig. 3, electrons are transferred into the polymer segment to reach a new equilibrium for the system. Instead of forming extended electronic waves, the extra electrons in the polymer form localized charged bipolarons. Figure 3(a) shows the displacements of lattice sites, from which we see that, in this case, three complete bipolarons are formed within the polymer together with some local distortions at the interface. The corresponding charge and spin distributions are shown in Fig. 3(b). In the present BK model for the nondegenerate polymer, bipolarons are energetically lower than polarons. Since each bipolaron has two confined electronic charges with opposite spins, a bipolaron has no spin. There is neither localized nor extended spin distribution within the polymer layer. Because the polymer is nonmagnetic in the ground state, or more generally at thermal equilibrium, there is no spin distribution far from the interface.

#### IV. FERROMAGNETIC CMR/POLYMER JUNCTION

Here, we consider the polymer chain in contact with a half-metallic ferromagnetic  $\text{Re}_{1-x}\text{Ak}_x\text{MnO}_3$  chain with electron concentration  $y = 0.32$ . By adjusting the relative chemical potential, electrons are transferred between the CMR material and polymer. At  $\mu_p = 2.15$  eV, there is essentially no electron transfer between the segments. Figure 4(a)

shows the displacements of the atoms (Mn, O and C) compared to their uniform bulk positions. Within the CMR segment, both the manganese and oxygen atoms are only slightly displaced. The small displacements are due to the finite length of the segment and disappear as the segment length is increased. The carbon atoms have a displacement of 0.05 Å, corresponding to the bulk dimerization of the polymer chain. The interfacial atoms have a deviation from the bulk dimerization, which results in a small expansion of the end bonds of the CMR segment and a contraction of the first few polymer bonds. The charge and spin densities are shown in Fig. 4 (b). Because the CMR material is completely spin polarized, the charge and spin densities coincide in this segment. The distributions of charge and spin density in each segment are uniform except for a small modulation near the interface. The modulation in the CMR material is a finite size effect discussed previously. There is neither a net charge nor spin distribution within the bulk polymer. When we increase the chemical potential of the CMR material, electrons are transferred into the polymer. The results for  $\mu_p = 2.90$  eV are shown in Fig. 5. At this value for the chemical potential, 6.11 electrons transfer to the polymer segment. The CMR segment keeps a nearly uniform lattice structure except a small deviation at the interface. In the polymer, from the displacements shown in Fig. 5 (a), bipolaron states form. The localized electronic density can be seen more clearly in Fig. 5 (b). Because the transferred electrons form spinless bipolarons, there is no spin amplitude within the polymer segment.

These results become more apparent if we examine the change in electronic density of states (DOS) defined by the Lorentz line shape formula

$$g(\epsilon) = \sum \frac{1}{(\epsilon - \epsilon_n)^2 + \gamma^2/4}; \quad (15)$$

where  $\epsilon_n$  is a one-electron energy eigenvalue and  $\gamma$  a phenomenological Lorentz line width, which we choose as  $\gamma = 0.15$  eV. Figure 6 (a) shows the DOS for the CMR/polymer chain before coupling of the two segments (that is, for the two separate material segments) and Fig. 6 (b) shows the DOS after coupling. The relative chemical potential was adjusted to be  $\mu_p = 2.15$  eV as in Fig. 4 so that there is no electron transfer between the CMR material

and polymer after coupling. From the figure we see that there is still a large gap for the spin down states, but the gap for spin up states decreases after coupling. All the occupied states near the Fermi level have spin up and these states are confined in the segment of the CMR material. Increasing the relative chemical potential  $\mu_p = 2.90$  eV as in Fig. 5, we plot the DOS before and after coupling in Fig. 7(a) and Fig. 7(b), respectively. Because the Fermi level of the CMR is above the bipolaron level of the polymer, electrons transfer to the polymer after coupling. They form double-charged bipolarons. The bipolaron levels are indicated in Fig. 7(b), where the levels of spin up and down states overlap (the spin up states of the bipolaron near 2.5 eV cannot be seen easily due to the large DOS caused by the CMR material). Thus, bipolarons have no spin. The difference in DOS of spin up and down at the bipolaron states arises from the effect of the CMR material at the interface.

## V. CONCLUSIONS

Organic ( $\pi$ -conjugated) polymers differ from traditional inorganic semiconductors due to their strong electron-lattice interactions. Carriers in (nondegenerate) polymers are not typically electrons or holes but rather charged polarons or bipolarons. In this paper we have studied the ground state properties of a ferromagnetic metal/organic polymer junction. Two kinds of magnetic contacts were considered, a simple ferromagnetic metal with fractional spin polarization and a CMR ferromagnet with a half-metallic ground state. It was found that the electric charges in the polymer near the interface can have spin polarization. The spin density decays in an oscillatory fashion into the polymer. By adjusting the relative chemical potential, electrons can be transferred into the polymer from the magnetic layer through the interfacial coupling. The transferred electrons form bipolarons, which have no spin, so that there is no spin density in the bulk of the polymer. The polymer is nonmagnetic and in the ground state, or more generally at thermal equilibrium, there will not be a spin polarization in this material far from the interface.

The present model is simple and only static characteristics were investigated. In addition,

the model is one-dimensional and Coulomb interactions between electrons were not included so that there was no Schottky effect at the interface. But major factors have been included, such as lattice relaxation and interfacial coupling. The main motivation for this model came from recent polarized spin injection (and spin-coherent transfer) experiments on the conjugated organic oligomer sexithienyl (thin film) in which a half-metallic ferromagnetic CMR contact was used [6]. This oligomer can serve as an active transport material for potential organic opto-electronic and spintronic devices. Dynamics under external bias will be studied to describe spin injection and polarized spin transport in conjugated organic materials, but an understanding of ground state properties is required to initiate a study of such dynamics.

## V I. A C K N O W L E D G M E N T

This work was supported by the SPINs program of the Defense Advanced Research Projects Agency and in part by the U.S. Department of Energy.

## REFERENCES

- [1] M. N. Baibich, J. M. Broto, A. Fert, F. Nguyen Van Dau, F. Petro, P. Etienne, G. Creuzet, A. Friederich, and J. Chazelas, *Phys. Rev. Lett.* **61**, 2472 (1988).
- [2] R. Meservey, *Phys. Rev. Lett.* **25**, 1270 (1970).
- [3] M. Johnson and R. H. Silsbee, *Phys. Rev. Lett.* **55**, 1790 (1985).
- [4] F. G. Monzon, H. X. Tang, and M. L. Roukes, *Phys. Rev. Lett.* **84**, 5022 (2000).
- [5] Y. Ohno, D. K. Young, B. Beschoten, F. Matsukura, H. Ohno, and D. D. Awschalom, *Nature* **402**, 790 (1999).
- [6] V. Dediu, M. Murgia, S. Barbanera, and C. Taliani, *AP Conf. Proc.* **591**, 548 (2001); V. Dediu, M. Murgia, F. C. Matocotta, S. Barbanera, and C. Taliani, *cond-mat/0104165*.
- [7] P. C. van Son, H. van Kempen, and P. Wyder, *Phys. Rev. Lett.* **58**, 2271 (1987).
- [8] G. Schmidt, L. W. Molenkamp, A. T. Filip, and B. J. van Wees, *cond-mat/9911014*.
- [9] I. Zutic, J. Fabian, and S. Das Sarma, *Phys. Rev. Lett.* **88**, 066603 (2002).
- [10] E. I. Rashba, *Phys. Rev. B* **62**, R16267 (2000).
- [11] D. L. Smith and R. N. Silver, *Phys. Rev. B* **64**, 045323 (2001).
- [12] J. D. Albrecht and D. L. Smith, *cond-mat/0202131*.
- [13] G. Schmidt, D. Ferrand, L. W. Molenkamp, A. T. Filip, and B. J. van Wees, *Phys. Rev. B* **62**, R4790 (2002).
- [14] M. Muccini, M. Schneider, and C. Taliani, *Synth. Met.* **116**, 301 (2001).
- [15] K. W aragai, H. A kim ichi, S. Hotta, H. Kano, and H. Sakaki, *Phys. Rev. B* **52**, 1786 (1995).
- [16] S. A. Brazovskii and N. N. Kirova, *Pis'ma Zh. Eksp. Teor. Fiz.* **33**, 6 (1981) [*JETP Lett.* **33**, 6 (1981)].

6, 4 (1981)].

[17] S.J.Xie, L.M.Mei, and D.L.Lin, Phys.Rev.B 50, 13364 (1994).

[18] See, e.g., S. Jin et al., Science 264, 413 (1994); A.J.Millis, Nature 392, 147 (1998);  
M.B.Salamon and M.Jaime, Rev.Mod.Phys. 73, 583 (2001).

[19] K.H.Ahn and A.J.Millis, Phys.Rev.B 61, 13545 (2000).

[20] A.J.Heeger, S.Kivelson, J.R.Schrieffer, and W.P.Su, Rev.Mod.Phys. 60, 781 (1988).

# FIGURES

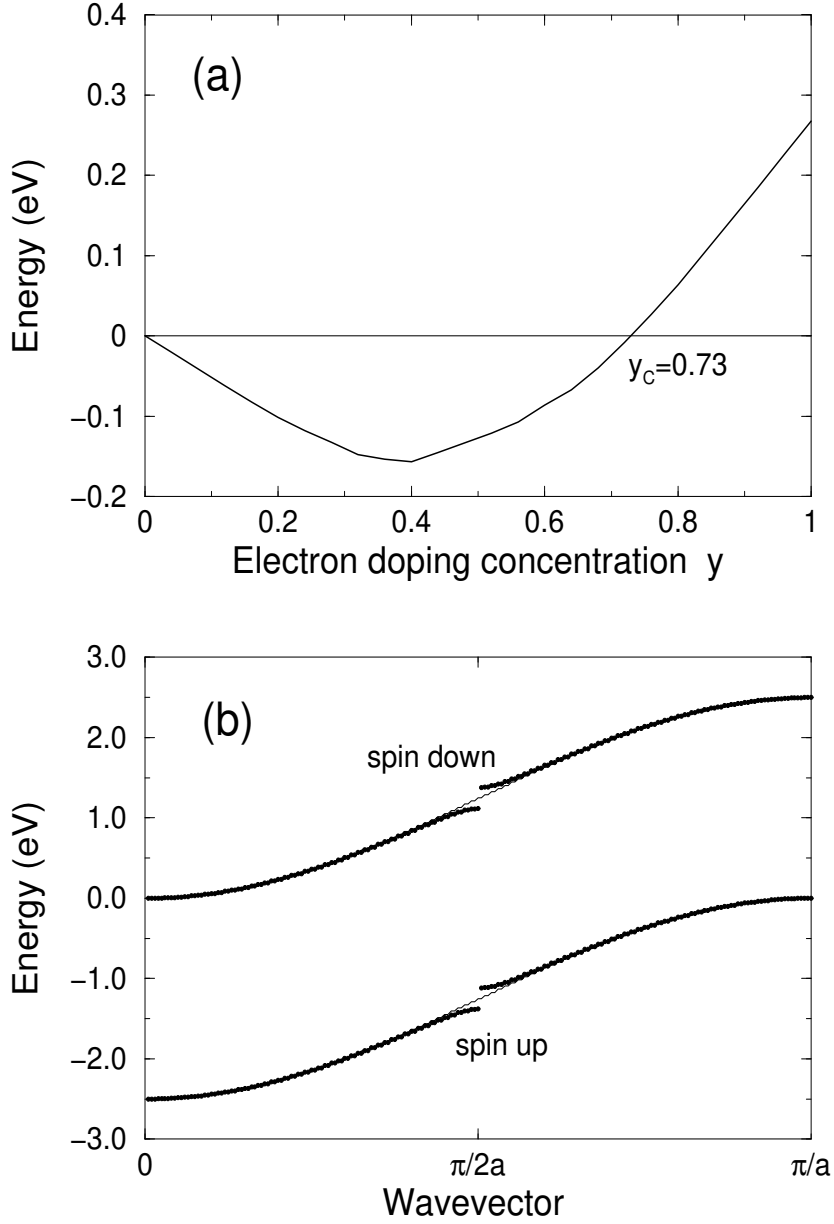


FIG .1. (a) Dependence of energy difference per site between a one-dimensional ferromagnetic chain and an antiferromagnetic  $\text{Re}_{1-x}\text{A}_x\text{K}_x\text{MnO}_3$  chain with doping concentration  $y$ . (b) Energy levels of  $\text{Re}_{1-x}\text{A}_x\text{K}_x\text{MnO}_3$  in the ferromagnetic state:  $y = 0.5$  (thick line) and  $y = 0.32$  (thin line). The upper curve in panel (b) is for spin down electrons and the lower curve is for spin up electrons. A gap of 0.26 eV appears at  $k = \pi/2a$  in the case of half doping ( $y = 0.5$ ).

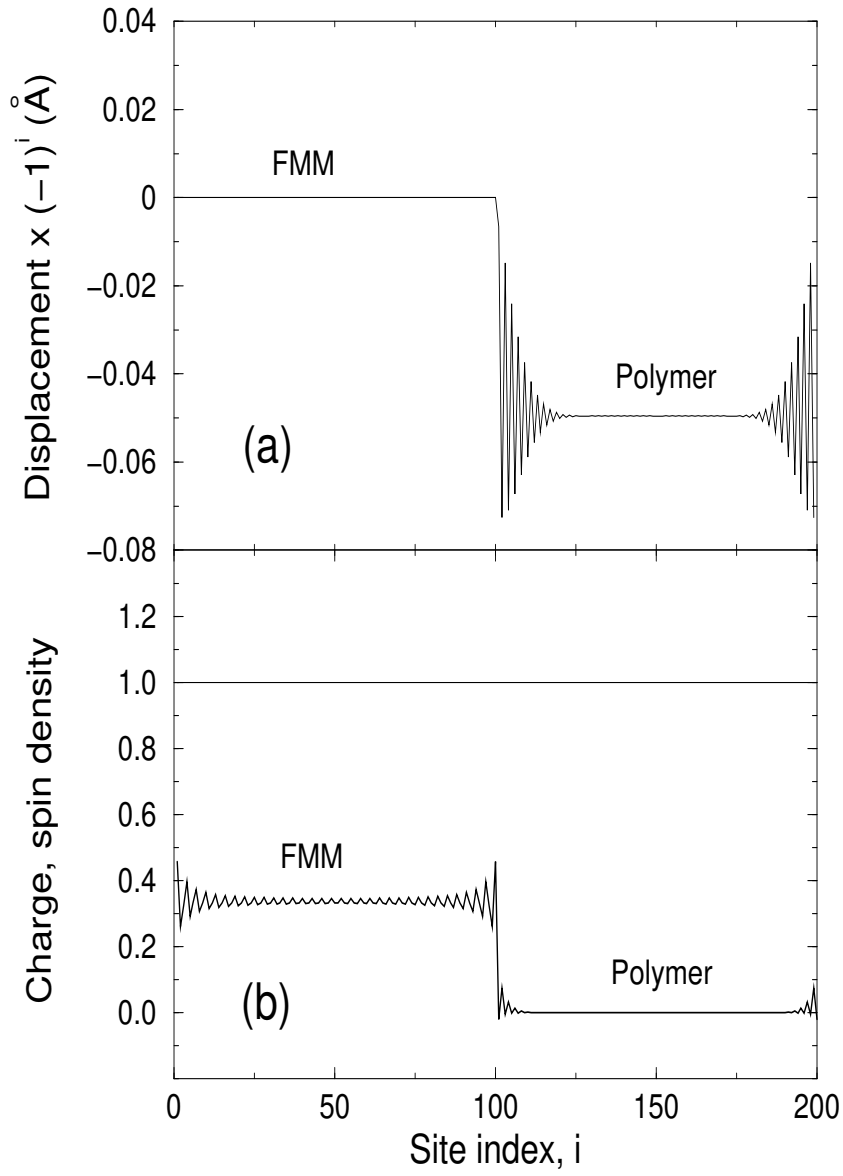


FIG .2. For a simple ferromagnetic metal (FMM)/polymer chain: (a) Site displacements; (b) charge (thin line) and spin (thick line) density distributions. There is no electron transfer between the FMM and the polymer. The interface is between sites 100 and 101 and  $p_p = 0$ . All the site displacements are plotted after multiplying with a factor  $(-1)^i$ , where  $i$  is the site index.



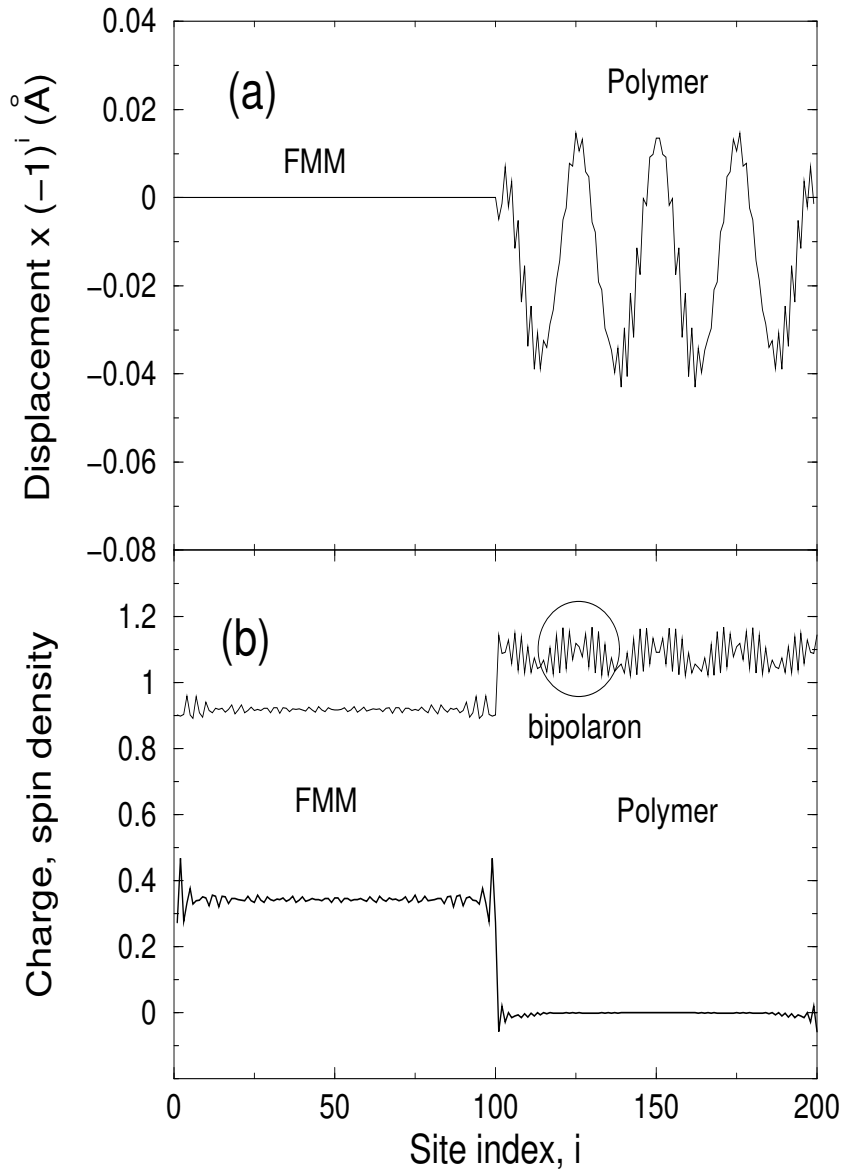


FIG. 3. Same as in Fig. 2 but for  $\mu_p = 1.0$  eV. Electrons are transferred from the FMM to the polymer through the interface by increasing the chemical potential of the FMM, resulting in bipolarons forming in the polymer.

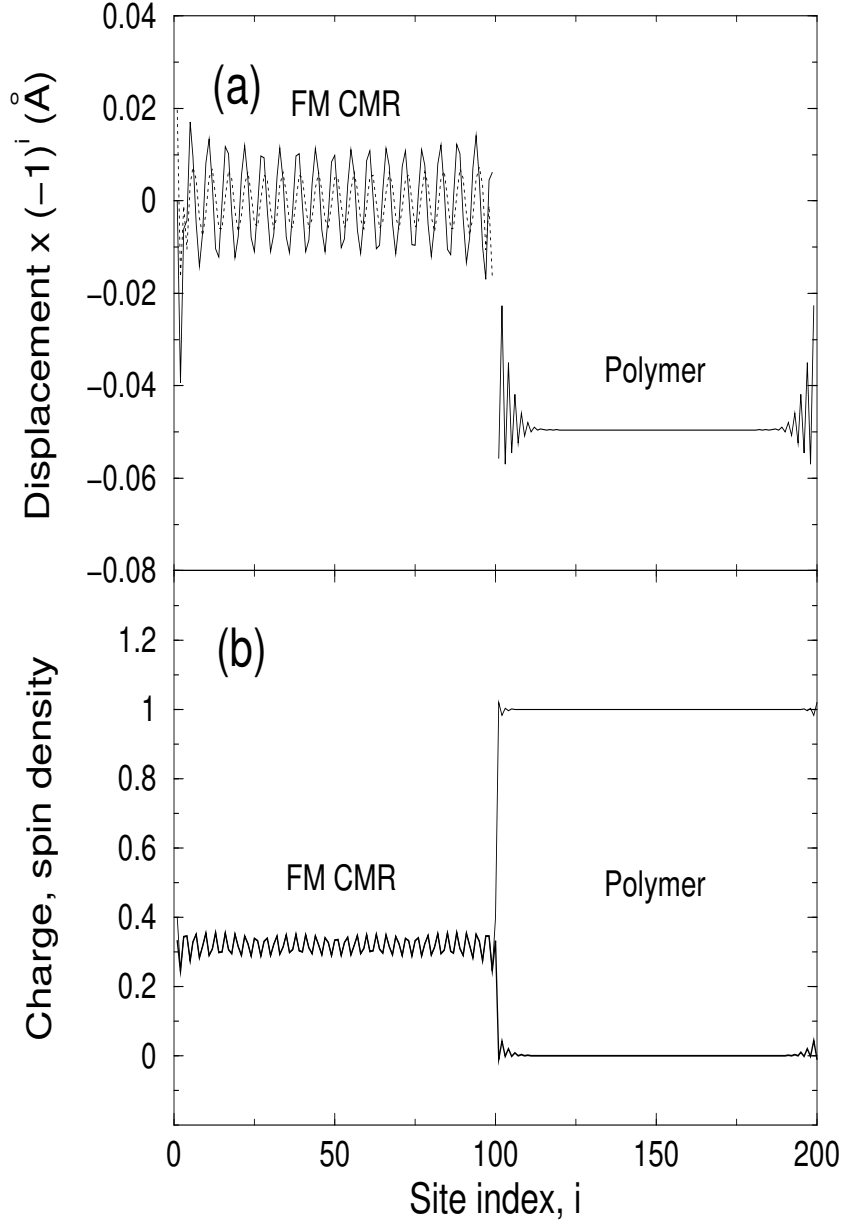


FIG. 4. For a ferromagnetic  $\text{Re}_{1-x}\text{Ak}_x\text{MnO}$  (FM CMR)/polymer chain: (a) Site displacements of Mn (left dotted), O (left solid) and C (right solid) atoms; (b) charge (thin line) and spin (thick line) density distributions. The charge and spin densities coincide in the CMR material. There is no electron transfer between the FM and the polymer. The interface is between sites 100 and 101.

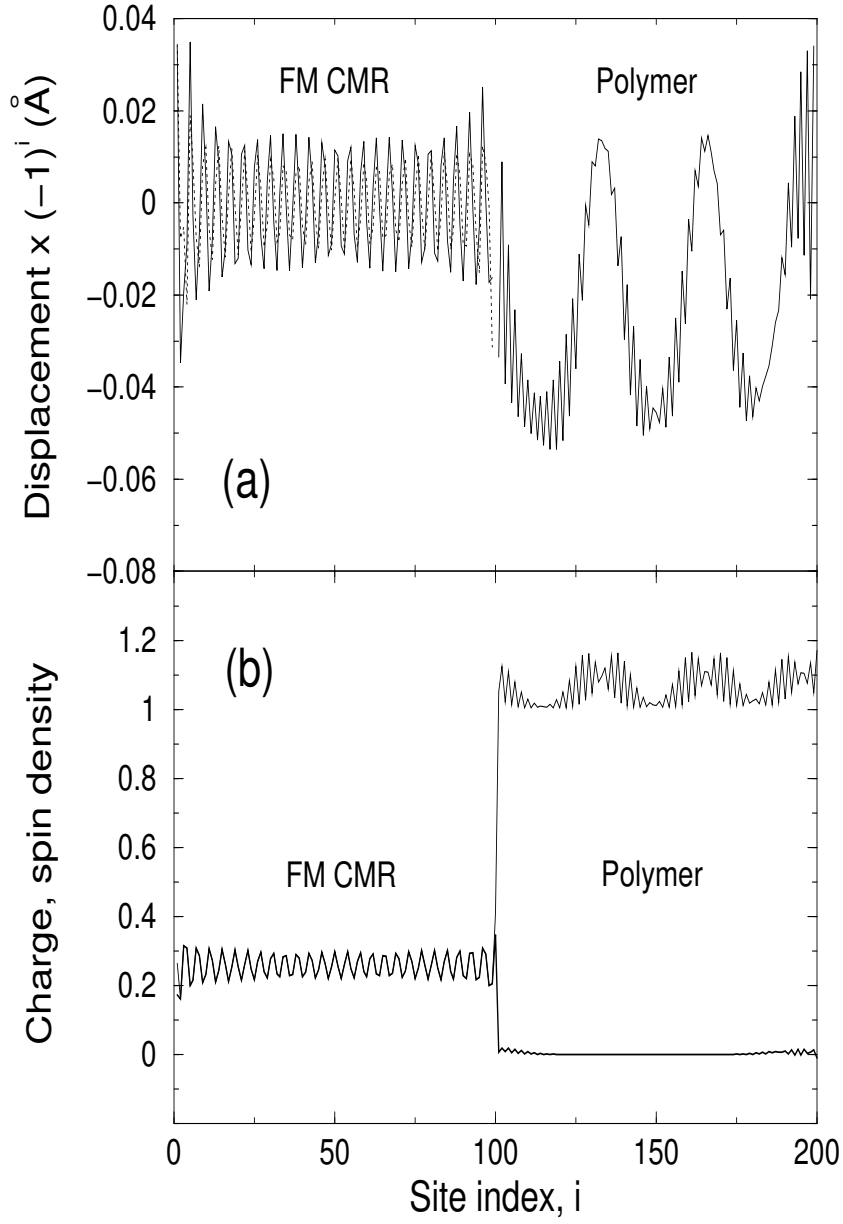


FIG. 5. Same as in Fig. 4 but with some electrons transferred from the FM CMR segment to the polymer through the interface by increasing the chemical potential of the FM CMR material, resulting in bipolarons forming in the polymer.

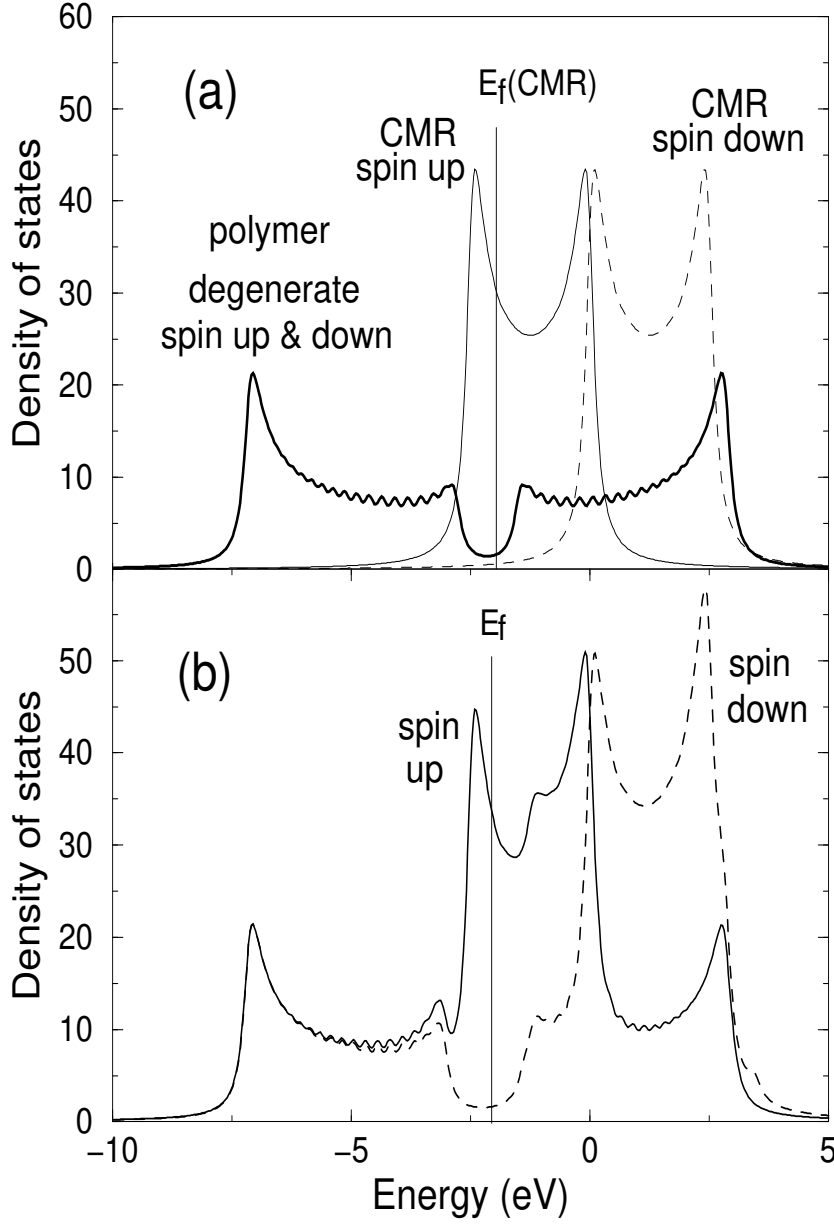


FIG . 6. Density of states of the FM CMR material and the polymer: (a) before coupling and (b) after coupling. The thick solid line in (a) is for both spin up and spin down electrons in the polymer, the thin solid (dashed) line in (a) is for spin up (spin down) electrons in the polymer. The solid (dashed) line in (b) is for spin up (spin down) electrons. The phenomenological Lorentz width is  $\gamma = 0.15$ . The Fermi level of the CMR material lies below the bipolaron energy of the polymer, so that there is no significant electron transfer.

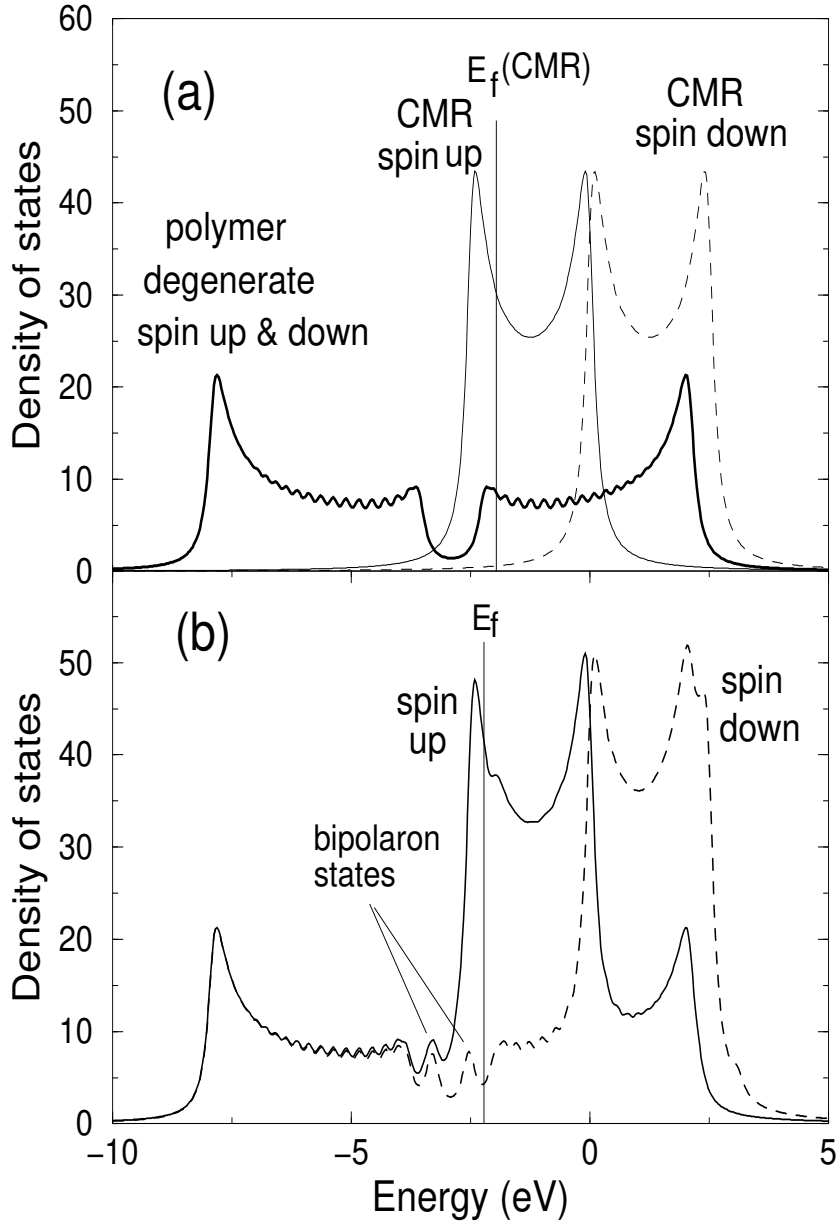


FIG. 7. Same as in Fig. 6 but with the Fermi level of the CMR material higher than the bipolaron energy of the polymer, so that electrons transfer from the CMR segment to the polymer after coupling.